Generalized kinetic potential in binary nucleation

Jin-Song Li
Course in Materials Science and Engineering, Graduate School of University of Tokushima, 2-1 Minamijosanjima, Tokushima 770-8506, Japan

Kazumi Nishioka*
Department of Optical Science and Technology, University of Tokushima, 2-1 Minamijosanjima, Tokushima 770-8506, Japan

Igor L. Maksimov
Faculty of Applied Physics and Microelectronics, Nizhny Novgorod University, 23 Gagarin Avenue, Nizhny Novgorod 603000, Russian Federation

(Received 3 February 1998; revised manuscript received 11 August 1998)

By introducing a coordinate transformation, we investigate the feature of a generalized kinetic potential for binary nucleation that governs the pathway of the major nucleation flux. The general conditions under which the major nucleation flux bypasses the thermodynamic saddle point are clarified, and both the discrepancy in the attachment rates of the two species and the nonuniformity of the direction of the nucleation flux are found to be the major causes of the bypassing. The ridge crossing phenomenon is explained on the basis of the present theory. Binary nucleation reduces consistently to single component nucleation when the attachment rate for one of the species tends to vanish. The present theory agrees with the results of numerical simulations. [S1063-651X(98)05612-8]

PACS number(s): 64.60.Qb, 05.20.Dd, 82.20.Db

I. INTRODUCTION

The problem of nucleation flux trajectories has recently attracted much attention in the physics community. A general approach to a feasible solution for multicomponent nucleation was outlined first by Langer [1]. His approach was based on the concept of the lowest intervening saddle point of the system's multidimensional free energy through which the major nucleation flux passes, thus driving the system from a metastable state to a state of greater stability. This concept was shown to be very fruitful. Since then many attempts have been made in order to demonstrate the kinetic pathway in a wide class of physical and chemical systems (see, e.g., Ref. [2] and references therein). The relevance of the binary nucleation flux topology with regard to acid rain phenomena was extensively discussed in a recent review [3]. Recently this approach was discussed in connection with the kinetic pathway problem in the segregation process [4,5], with the location of the real saddle point for nucleation during Martensitic transformation [6]. However, despite obvious progress in this direction, our comprehension of a technique for locating the pathways of the major nucleation flux in a specific multicomponent system is still lacking. In the present paper we make an attempt to answer this question for the case of binary nucleation.

Multicomponent nucleation is a very wide area of science and technology, with applications ranging from atmospheric science to materials science (for a review see Ref. [3], and references therein). The kinetics of binary nucleation was first considered by Reiss [7], who assumed that nucleation goes through the saddle point of the surface of the reversible work W^{rev} of forming a cluster [we call it a thermodynamic saddle point (TSP)], keeping a constant direction of the flux in the TSP region and following the path of the steepest descent of W^{rev}. Other theories [2,8–10], proposed later, are also based on the assumption that the major nucleation flux goes through the TSP with a constant direction, although Stauffer realized that the direction of growth will be affected by the asymmetry of the kinetic coefficients [10]. However, numerical results obtained by solving the kinetic governing equations showed that in some cases the major nucleation flux bypasses the TSP [11–13]. This phenomenon, referred to as ridge crossing, seems to be a possible phenomenon when the two condensation rates differ significantly. The nucleation across a ridge was studied by Trinkaus [14], Shi and Seinfeld [15], Wu [16], and Berezhkovskii and Zitserman [17], and they ascribed the ridge crossing phenomenon to coupling between the shape of the free energy surface and a large disparity in the impingement rates. However, in their treatments [14–17] the expansion of W^{rev} at the TSP is employed, so that their theories may be valid for only the vicinity of the TSP. Experimental observations also showed large discrepancy from the classical nucleation theory at low concentration of one of the species [18].

Basically, theories [2,7–10], despite their many successes, have been concerned with only the vicinity of the TSP. Moreover, these theories are not able to judge by themselves whether the major nucleation flux passes through the TSP region or not, since W^{rev} is determined by thermodynamic parameters only. Consequently, the kinetic potential W^{K} was introduced instead of W^{rev} as the relevant potential to determine the kinetic pathway of the nucleation flux. The kinetic potential includes both the thermodynamic and kinetic parameters, and the expression for the W^{K} reads [10,14,19]

*Deceased on 20 May 1998.

$$W^K = W^{\mathrm{rev}} + W_1, \tag{1}$$

$$W_1 = -kT \ln K_A^+, \tag{2}$$

where K_A^+ denotes the attachment rate of A species, T the temperature, and k the Boltzmann constant. However, it was shown recently [19] that the kinetic potential W^K by itself cannot determine unambiguously the pathway of the major nucleation flux. In the present paper, we provide a generalized kinetic potential that contains sufficient information to determine the pathway of the major nucleation flux.

The outline of the paper is as follows. First, we introduce a coordinate transformation where the nonuniformity of the direction of the nucleation flux is taken into account. By virtue of this transformation, the generalized kinetic potential, which governs the pathway of the major nucleation flux, can be separated into several terms that are subject to direct physical interpretations. Then we discuss the contribution of these terms to the generalized kinetic potential, and show their roles in determining the pathway of the major nucleation flux. Thus the general conditions for ridge crossing are clarified. Finally, a numerical example of the ridge crossing is explained in light of the present theory.

II. GENERALIZED KINETIC POTENTIAL

Consider the process of homogeneous nucleation of liquid clusters in a binary vapor, which we denote as the α phase, of species A and B at temperature T, pressure p^α and composition x_B^α of the species B. Suppose that the vapor is in metastable equilibrium and the driving force exists toward the stable liquid phase β. The basic equation governing the time dependent cluster concentration $f(n_A,n_B,t)$ may be written as [7]

$$\frac{\partial f(n_A,n_B,t)}{\partial t} = -\frac{\partial J_A(n_A,n_B,t)}{\partial n_A} - \frac{\partial J_B(n_A,n_B,t)}{\partial n_B}, \tag{3}$$

where n_i $(i=A,B)$ denotes the number of i molecules in a cluster. The components J_A and J_B of the nucleation flux $\mathbf{J}$ are given by [7]

$$J_A(n_A,n_B,t) = -c_0(n_A,n_B)K_A^+(n_A,n_B)\frac{\partial}{\partial n_A} \times \left(\frac{f(n_A,n_B,t)}{c_0(n_A,n_B)}\right), \tag{4}$$

$$J_B(n_A,n_B,t) = -c_0(n_A,n_B)K_B^+(n_A,n_B)\frac{\partial}{\partial n_B} \times \left(\frac{f(n_A,n_B,t)}{c_0(n_A,n_B)}\right), \tag{5}$$

where K_B^+ denotes the attachment rate of B species, and $c_0(n_A,n_B)$ the metastable equilibrium concentration of clusters specified by (n_A,n_B) in the system. $c_0(n_A,n_B)$ is given by

$$c_0(n_A,n_B) = \Phi_{\mathrm{LP}}(c_A+c_B)\exp[-W^{\mathrm{rev}}(n_A,n_B)/kT], \tag{6}$$

where Φ_{LP} denotes the Lothe-Pound factor [20] and c_i the number density of i species monomers in the vapor. We do not discuss here the value of Φ_{LP}, because it is not directly related to the main purpose of the present paper. We neglect the cluster size dependence of Φ_{LP} in the following. No explicit form of W^{rev} is needed in the following treatment. $K_i^+(n_A,n_B)$ may be given, under the approximation that the effective area for condensation is $4\pi R^2$, where R denotes the radius of a cluster characterized by (n_A,n_B), by

$$K_A^+(n_A,n_B) = 4\pi R^2(n_A,n_B)p_A^\alpha/(2\pi m_A kT)^{1/2}, \tag{7}$$

$$K_B^+(n_A,n_B) = 4\pi R^2(n_A,n_B)p_B^\alpha/(2\pi m_B kT)^{1/2}, \tag{8}$$

where m_i denotes the molecular mass of i species. Note that the ratio between $K_A^+(n_A,n_B)$ and $K_B^+(n_A,n_B)$ is constant for a given state of a parent vapor phase, i.e.,

$$r = \frac{K_B^+(n_A,n_B)}{K_A^+(n_A,n_B)} = \frac{p_B^\alpha}{p_A^\alpha}\left(\frac{m_A}{m_B}\right)^{1/2} = \text{const.} \tag{9}$$

Equation (3) represents the conservation of the number densities of clusters, and it holds when the cluster coalescence is negligible. This will be the case in the nucleation stage before the growth stage starts. Equations (4) and (5) show that the ''mobility coefficient'' matrix is not a unit matrix multiplied by a scalar. This ''anisotropy'' plays an important role in determining the pathway of the major nucleation flux.

Now we introduce a force vector field $\mathbf{V}=(V_A,V_B)$ derived from the potential $\Psi = f/c_0$ [10] as

$$\mathbf{V} = -\boldsymbol{\nabla}\Psi. \tag{10}$$

From Eqs. (4) and (5), $\mathbf{V}$ is related to $\mathbf{J}$ by

$$V_A(n_A,n_B,t) = \frac{J_A(n_A,n_B,t)}{c_0(n_A,n_B)K_A^+(n_A,n_B)}, \tag{11}$$

$$V_B(n_A,n_B,t) = \frac{J_B(n_A,n_B,t)}{c_0(n_A,n_B)K_B^+(n_A,n_B)}. \tag{12}$$

We represent the direction of $\mathbf{V}$ in the size space by an angle θ with respect to the n_A axis, i.e.,

$$\tan\,\theta(n_A,n_B,t) = V_B(n_A,n_B,t)/V_A(n_A,n_B,t). \tag{13}$$

By employing Eqs. (11) and (12), the relation between θ and the direction ϕ of nucleation flux is obtained by

$$\tan\,\theta(n_A,n_B,t) = \tan\,\phi(n_A,n_B,t)/r, \tag{14}$$

where

$$\tan\,\phi(n_A,n_B,t) = J_B(n_A,n_B,t)/J_A(n_A,n_B,t). \tag{15}$$

Figure 1 shows the relation between θ and ϕ for various values of r. When $r=1$, $\theta\equiv\phi$; when $r<1$, $\theta>\phi$, with the exception that $\theta=\phi$ at $\phi=0°$ and 90°; when $r\to 0$, the curve approaches the ordinate axis.

We introduce time-dependent orthogonal curvilinear coordinates ξ and η, in which ξ is chosen to be the lines of flow of the vector field $\mathbf{V}$ and η the contours of Ψ. $\delta\xi$ and $\delta\eta$ are related to δn_A and δn_B by [21]

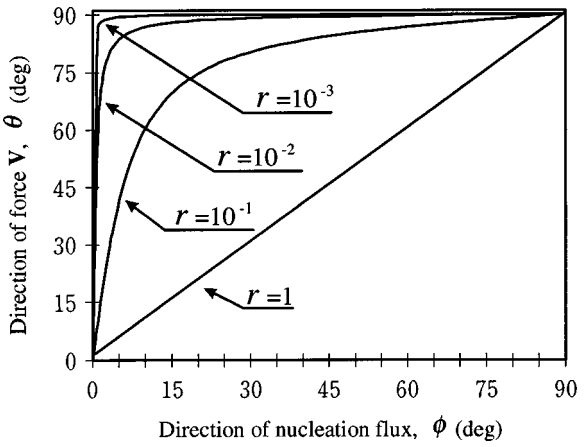

FIG. 1. The relation between θ and ϕ for various values of r.

$$\delta n_A = h_1 \delta\xi \cos\theta - h_2 \delta\eta \sin\theta, \tag{16}$$

$$\delta n_B = h_1 \delta\xi \sin\theta + h_2 \delta\eta \cos\theta, \tag{17}$$

where h_1 and h_2 denote the scale factors. By employing Eqs. (16) and (17), the force components $\partial\Psi/\partial n_A$ and $\partial\Psi/\partial n_B$ may be expressed as

$$\partial\Psi/\partial n_A = (\cos\theta/h_1)\partial\Psi/\partial\xi - (\sin\theta/h_2)\partial\Psi/\partial\eta, \tag{18}$$

$$\partial\Psi/\partial n_B = (\sin\theta/h_1)\partial\Psi/\partial\xi + (\cos\theta/h_2)\partial\Psi/\partial\eta. \tag{19}$$

From Eqs. (13), (18), and (19), we obtain

$$\partial\Psi/\partial\eta = 0, \tag{20}$$

i.e., Ψ is independent of η, hence $\Psi = \Psi(\xi,t)$. This automatically leads to a simple relation between the magnitude of $\mathbf{V}(V=|\mathbf{V}|)$ and $V_0 = -\partial\Psi(\xi,t)/\partial\xi$:

$$V = (1/h_1)V_0(\xi,t). \tag{21}$$

Substituting Eq. (21) into Eqs. (11) and (12), we obtain the following expressions for J_A and J_B:

$$J_A(n_A,n_B,t) = (1/h_1)V_0 c_0 K_A^+ \cos\theta, \tag{22}$$

$$J_B(n_A,n_B,t) = (1/h_1)V_0 c_0 K_B^+ \sin\theta. \tag{23}$$

The magnitude of the nucleation flux can be expressed as

$$J(n_A,n_B,t) = \Phi_{\mathrm{LP}}(c_A + c_B)\exp(-W^{\mathrm{GK}}/kT). \tag{24}$$

We call W^{GK} as the generalized kinetic potential that is given by

$$W^{\mathrm{GK}} = W^{\mathrm{rev}} + W_0 + W_1 + W_2 + W_3, \tag{25}$$

$$W_0 = -kT \ln V_0, \tag{26}$$

$$W_2 = kT \ln h_1, \tag{27}$$

$$W_3 = -\frac{kT}{2}\ln(\cos^2\theta + r^2\sin^2\theta) = -kT \ln(\cos\theta/\cos\phi). \tag{28}$$

To obtain the last expression for W_3 Eq. (14) is employed. As seen from Eq. (25) W^{GK} consists of the force term W_0, the kinetic term W_1, the scaling term W_2, and the anisotropy term W_3 as well as the thermodynamic reversible work W^{rev}.

Up to now, we do not make any approximation, so that Eqs. (22)–(24) are exact results that are valid for the whole size space and for transient nucleation. Since Eqs. (16) and (17) are a curvilinear transformation, the nonuniformity of the direction of nucleation flux is taken into account. In the theories of Reiss [7] and Stauffer [10], the uniformity of the direction of nucleation in the TSP region is assumed, and a linear coordinate transformation is employed in which one axis is chosen along the direction of the flux. This assumption precludes the variations of W_2 and W_3, of these W_3 turns out to be the major cause of ridge crossing (an example will be given later).

III. MAJOR NUCLEATION FLUX AND THE STRUCTURE OF W^{GK}

It follows from Eq. (24) that J is governed by W^{GK}. The pathway of the major nucleation flux is given by the valley of W^{GK}, since this corresponds to the ridge of the profile of J. Obviously, it does not pass through the TSP in general due to W_0, W_1, W_2, and W_3.

When the major nucleation flux bypasses the TSP, it has been called the ridge crossing of W^{rev} [13,14]. The physical origin of the ridge crossing phenomenon can be ascertained by analyzing the topology of the surface $W^{\mathrm{GK}}(n_A,n_B)$. Since the major nucleation flux goes along the valley of W^{GK}, it inevitably goes across the ridge of the surface of $W^{\mathrm{rev}}(n_A,n_B)$. In the conventional picture this is interpreted as ridge crossing. Now let us discuss the contributions of W_0, W_1, W_2, and W_3 to the pathway of the major nucleation flux.

A. Force term W_0 and kinetic term W_1

The force term W_0 is a function that is independent of η, i.e., along an η line it is constant. If the scale for the coordinate ξ is properly chosen, V_0 can be a constant. For example, if we assign

$$\xi = 1 - \Psi, \tag{29}$$

it follows that

$$V_0 = 1. \tag{30}$$

In the following treatment we employ this choice for ξ, so that W_0 is zero.

When W_1 is added to W^{rev}, it is called the kinetic potential W^K [19,22,23]. The main feature of the surface of W^K can be described by the kinetic critical nucleus [19,22,23], for which the probabilities of its decay and growth balance, i.e.,

$$K_A^+ = K_A^-, \tag{31}$$

$$K_B^+ = K_B^- . \tag{32}$$

The saddle point and extremum on the surface of W^K correspond to the kinetic critical nucleus n^K. In Ref. [19], the kinetic critical nucleus was extensively discussed for binary systems, and it was shown there that (1) the size n^K of the kinetic critical nucleus is in general smaller than the size n^* of the thermodynamic critical nucleus; (2) there exist two values $n^{K(1)}$ and $n^{K(2)}$ for n^K; and (3) beyond the critical state, n^K does not exist, and it is called the runaway instability. In this case, there is no saddle point or extremum on the surface of W^K. In the present paper, we do not consider the case of the runaway instability. Note that the kinetic term W_1 varies strongly with size for small clusters, but varies weakly for larger ones. When the driving force for nucleation is not very large, $n^{K(1)}$ will be large, and W_1 may be approximately treated as a slightly tilted plane added to the surface of W^{rev} for not small size, so that $n^{K(1)}$ will be a saddle point on W^K which we call the kinetic saddle point (KSP). The numerical results [19] show that the difference in size between the TSP and KSP is negligibly small for the systems treated by Wyslouzil and Wilemski [13], so that W_1 is not the major cause of the ridge crossing that is found by Wyslouzil and Wilemski.

B. Scaling term effect on the pathway of the major nucleation flux

Since the scale factor can be obtained only when the governing equation is solved, in the present case W_2 is an unknown term. However, in determining the pathway of the major nucleation flux, only the variation of W_2 is needed, so that we may make an approximation for the variation of W_2. Let us consider contour lines of W^{GK} in the size space, then the valley corresponds to the trajectory of the extrema of the curvature along the contour lines of W^{GK}. However, the equation to determine it is too complicated to be useful in a numerical study. The possible way to approximately determine the valley is to select a coordinate system, thus the trajectory of the extrema along grids of one coordinate approximately gives the valley of W^{GK}. It becomes the exact result when W^{GK} along the valley is constant, and it is a good approximation when the valley is sharp. In the present paper, we chose the curve of

$$\partial W^{\text{GK}} / \partial \eta = 0 \tag{33}$$

as an approximation to the valley of W^{GK}, since the numerical results [12,13] showed that the magnitude of nucleation flux dominates within a narrow region along the pathway of the major nucleation flux and changes very slowly along it; hence the curve determined by Eq. (33) is close to the valley of W^{GK} in these cases. In the following discussion we limit our consideration to the cases where the curve determined by Eq. (33) approximately gives the valley of W^{GK}.

As we see from Eq. (19), the scale factor h_1 represents the relative magnitude of force $\mathbf{V}$ along an η line, and the minimum of h_1 corresponds to the largest value of $\mathbf{V}$ on this curve. The variation of h_1 with η can be expressed by [21]

$$\partial \mathbf{a}_2 / \partial \xi = (\mathbf{a}_1 / h_2) \partial h_1 / \partial \eta, \tag{34}$$

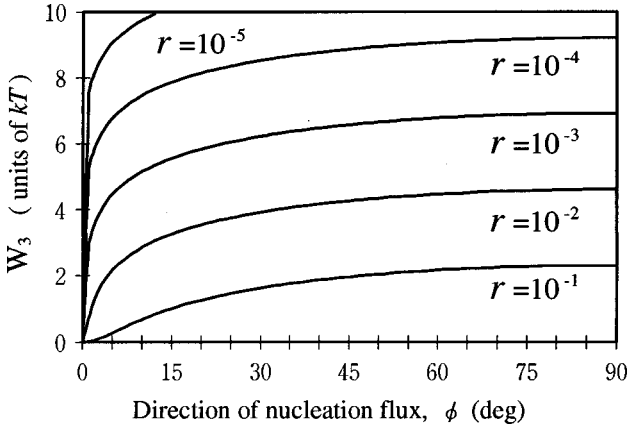

FIG. 2. The values of W_3 with ϕ for various values of r.

where $\mathbf{a}_1$ and $\mathbf{a}_2$ denote the unit vectors along ξ and η coordinates, respectively. The transformation from $(\mathbf{n}_A, \mathbf{n}_B)$ to $(\mathbf{a}_1, \mathbf{a}_2)$ can be expressed by

$$\mathbf{n}_A = \mathbf{a}_1 \cos\theta - \mathbf{a}_2 \sin\theta, \tag{35}$$

$$\mathbf{n}_B = \mathbf{a}_1 \sin\theta + \mathbf{a}_2 \cos\theta, \tag{36}$$

where $\mathbf{n}_A$ and $\mathbf{n}_B$ denote the unit vectors along n_A and n_B coordinates. From Eqs. (34), (35), and (36), we can obtain

$$\partial h_1 / \partial \eta = -h_2 \partial\theta / \partial \xi. \tag{37}$$

Then, the variation of W_2 with η can be rewritten as

$$\partial W_2 / \partial \eta = -kT (h_2 / h_1) \partial\theta / \partial \xi. \tag{38}$$

Since θ represents the direction of the tangent to ξ lines (η = const), when ξ lines are relatively straight, i.e., $(1/h_1)\partial\theta/\partial\xi \approx 0$, $(1/h_2)\partial W_2/\partial\eta$ will be small. It is interesting that Wyslouzil and Wilemski [24] found that the η lines form a set of approximately straight and parallel lines for the ethanol-hexanol system, and this qualitative behavior does not seem to depend on the specific values of the impingement rates. These numerical results imply that h_1 is approximately constant along each η line, hence $\partial W_2/\partial\eta$ can be neglected for these cases. It should be noted that almost constant θ along an η line does not necessarily mean that ϕ is also almost constant, which can be seen in Fig. 1.

C. Anisotropy term and the ridge crossing phenomenon

It follows from Eqs. (12) and (27) that

$$W_3 = -\frac{kT}{2} \ln \frac{r^2(1+\tan^2\phi)}{r^2+\tan^2\phi}. \tag{39}$$

Figure 2 shows variation of the anisotropy term W_3 with ϕ for various values of r. In general, W_3 increases with ϕ from the minimum value of zero for $\phi = 0$ to the maximum value $-kT \ln r$ for $\phi \to \pi/2$. When r is small, W_3 increases rapidly with ϕ for small ϕ and gradually for large ϕ. When r approaches zero, the curve of W_3 approaches the ordinate axis for small ϕ. From the first expression for W_3 in Eq. (28) we can obtain the variation of W_3 with θ for various values of r as shown in Fig. 3. The variations of W_3 depend on r

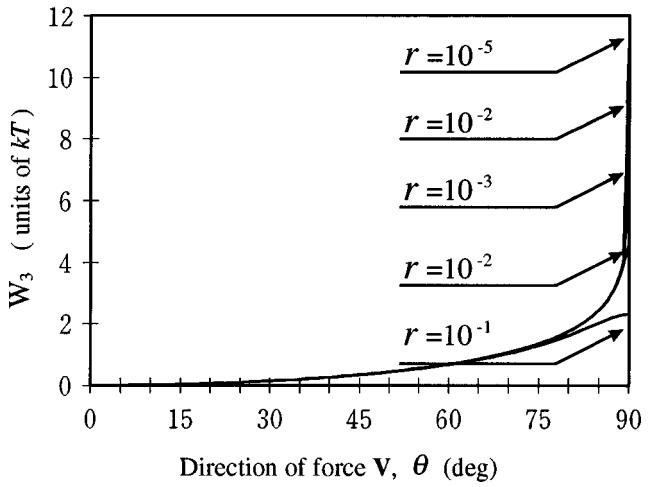

FIG. 3. The values of W_3 with θ for various values of r.

strongly when θ is close to 90°, but weakly on r for smaller values of θ. When θ is small, $\cos^2\theta$ dominates and W_3 becomes independent of r. However, when θ is close to 90°, $r^2\sin^2\theta$ dominates, and hence W_3 depends strongly on r.

Consider the cases in which ϕ decreases (i.e., θ decreases) monotonically along η lines, where η is chosen to increase from the n_B axis toward the n_A axis. Then, W_3 decreases monotonously along an η line. Figure 4 shows a schematic variation of W^{GK} along an η line by neglecting the variations of W_1 and W_2. The minimum of W^{rev} is denoted by C. When W_3 is added to W^{rev}, the minimum is shifted to D. Note that the value of η corresponding to D is larger than that corresponding to C. That is, the curve determined by $\partial W^{\mathrm{GK}}/\partial\eta=0$ is shifted away from the n_B axis and is bent toward the n_A axis compared with the curve determined by $\partial W^{\mathrm{rev}}/\partial\eta=0$; hence it does not pass through either the KSP or TSP.

It should be emphasized again that the above discussion is based on the variation of the direction of the nucleation flux along an η line. Once the direction of the nucleation flux is assumed to be constant in the TSP region [2,7–10], the variations of W_2 and W_3 are entirely excluded, so that the major cause of ridge crossing is omitted.

Thus, the anisotropy term W_3 plays the central role in judging whether the major nucleation flux passes through the TSP or not. When the variation of W_3 can be neglected compared with that of W^{rev}, the conventional Reiss assumption that the major nucleation flux passes through the TSP may be a good approximation. It may be valid under the following cases: (1) smooth variation of the anisotropy term: $\partial(W_3/W_{3\,\max})/\partial\phi<1$, which is relevant for $r>0.1$ (see Fig. 2 of the present paper and Fig. 2(a) in Ref. [13]); (2) the variation of W^{rev} with η is sharp in comparison to the variation of W_3, i.e., W^{rev} takes a sharp extremum at the TSP (see Fig. 5 in Ref. [12]); and (3) ϕ is approximately constant along η ($\partial\phi/\partial\eta\approx0$), e.g., flux trajectories are parallel and straight (see Fig. 3 in Ref. [13]).

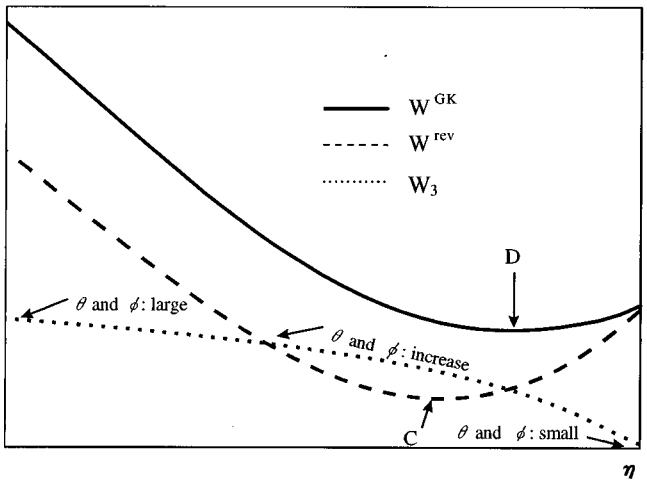

FIG. 4. Schematic changes of W^{rev}, W_3, and W^{GK} with η. The direction of η is chosen so that θ and ϕ tend to decrease with η.

The ridge crossing of W^{rev} will be observed only when r is small enough. For small enough r the pathway of the major nucleation flux may be shifted far away from the TSP. When this happens, the flux trajectories inevitably go across the ridge lines of the surface of $W^K(n_A,n_B)$ as well as of $W^{\mathrm{rev}}(n_A,n_B)$. If the region around the TSP is relatively flat and the direction of the nucleation flux varies strongly in the TSP region, the ridge crossing may also be observed even for not very small r ($r\approx0.01$). The ridge crossing found by Greer *et al.* [11] and Wyslouzil and Wilemski [13] are likely to correspond to this case.

The ridge crossing found by McGraw [12] in the water–sulfuric-acid system may be an example of the highly anisotropic case. Since W^{rev} is very sharp on the TSP, the major nucleation flux passes through the TSP and follows the narrow valley of W^{rev} even for highly supersaturated (200% relative humidity) water vapor condition, i.e., for small values of r [12]. However, when r is further decreased (in the order of 10^{-14}), ridge crossing is observed.

D. Transition to unary nucleation

The anisotropy term W_3 also plays the central role in the transition from binary to unary nucleation. When the concentration c_B of B species in a binary parent phase decreases, the TSP moves toward the n_A axis, and when $c_B/c_A\to0$, the TSP approaches the n_A axis. When $c_B/c_A=0$, i.e., $c_B=0$, the TSP is located on the n_A axis. This is the thermodynamic process of transition to unary nucleation and it is controlled by the thermodynamic parameter c_B/c_A. On the other hand, when r decreases, J_B/J_A decreases and ultimately $J_A(n_A,n_B>0,t)$ as well as $J_B(n_A,n_B>0,t)$ become negligible compared with $J_A(n_A,0,t)$ on the n_A axis. This is the kinetic process of the transition to unary nucleation, and it is controlled by the kinetic parameter r. Although $c_B/c_A\to0$ as well when $r\to0$, the physical roles of these two parameters in the transition are different. The theories [2,7–10] of binary nucleation based on the assumption that the major nucleation flux passes through the TSP are not consistent in dealing with the transition to unary nucleation, since the thermodynamic parameter alone is assumed to determine the pathway of the major nucleation flux.

Consider highly anisotropic cases, i.e., small values of r. The anisotropy term W_3 reflects the role of the kinetic parameter r, and it prevents the major nucleation flux from going toward the $\mathbf{n}_B$ axis. As we see in Fig. 2, when r becomes small, W_3 increases steeply with ϕ for small ϕ. Accordingly, point D in Fig. 4 shifts toward the point corresponding to a small value of ϕ, since even very small

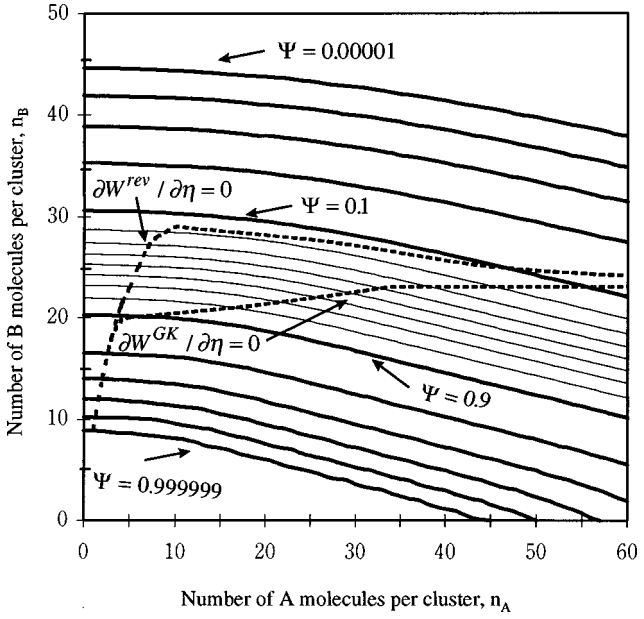

FIG. 5. Contours of Ψ and the pathway of the major nucleation flux. The light solid lines are in the step of 0.1. The heavy contour lines below the light solid lines correspond to the increase in the value of $1-\Psi$ by a ratio of 10, and the heavy solid lines above the light solid lines to the decrease in the value of Ψ by a ratio of 10 from 10^{-1} to 10^{-5}.

deviation from this angle results in a rapid increase in W^{GK}. When r is small enough, W_3 dominates in locating the minimum of W^{GK} along η lines and it occurs at $\phi \approx 0$. In this case, the valley of W^{GK} coincides with the n_A axis, i.e., the transition from binary nucleation to unary nucleation occurs.

IV. A NUMERICAL EXAMPLE OF RIDGE CROSSING

Let us consider as an example the ridge crossing reported by Wyslouzil and Wilemski [13]. Figure 5(b) in their paper [13] shows that the major nucleation flux bypasses the TSP for one specific vapor-liquid system (PD2) when r is about $\frac{1}{54}$. We repeat their calculation with the same conditions in order to obtain the contours of Ψ and the exact values of ϕ. Our numerical results are similar to that reported by Wyslouzil and Wilemski, i.e., the major nucleation flux bypasses the TSP, as shown in Fig. 5(b) of their paper [13]. Figure 5 shows the contours of Ψ obtained from our numerical results. As illustrated in Fig. 5, the contours form a set of nearly parallel but *curved* lines, which are different from that for the ideal ethanol-hexanol system where the contours show a set of nearly parallel and *straight* lines and the major nucleation flux passes through the TSP [24]. For the ideal ethanol-hexanol case, the features of the contours imply that the variations of both W_2 and W_3 along an η line can be neglected, so that the major nucleation flux passes through the TSP. However, for the PD2 case, the variation of W_3 cannot be neglected, since the curvature of the contours means the variation of θ. By employing [21]

$$h_1 = \left(\frac{\partial n_A}{\partial \xi} \right) \sin\, \theta, \tag{40}$$

Eqs. (28) and (26), W_2 can be calculated. With the help of

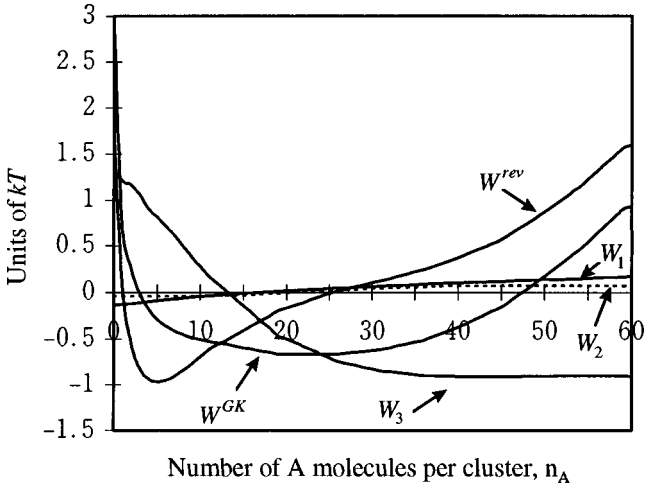

FIG. 6. The values of W^{GK}, W^{rev}, W_1, W_2, and W_3, each of which indicates the value after its average over η is subtracted, along the η line corresponding to $\Psi = 0.6$.

Eq. (33), we determine the pathway of the major nucleation flux that is superimposed in Fig. 5 as well as the valley of W^{rev}. In the region with $\Psi > 0.9$, the variation of W^{rev} dominates so that the pathway of the major nucleation flux practically coincides with the valley of W^{rev}; in the region with $0.1 < \Psi \leqslant 0.9$, the variation of W_3 is comparable with that of W^{rev}, so that the pathway of the major nucleation flux is bent towards the n_A axis; in the region with $\Psi < 0.1$, the pathway of the major nucleation flux approaches again the valley of W^{rev}. Along η lines, we do find that the variations of W_1 and W_2 are negligibly small compared with that of W^{rev} and W_3. A typical case corresponding $\Psi = 0.6$ is shown in Fig. 6.

VI. SUMMARY

Binary nucleation from vapor to liquid phase was studied, and the following results obtained.

(1) Introducing a curvilinear coordinate system, we investigated the feature of a generalized kinetic potential that governs the pathway of the major nucleation flux.

(2) The major nucleation flux does not in general pass through either the thermodynamic or the kinetic saddle point, but it may not easy to be observed for most vapor-liquid systems (see Ref. [13]). General conditions under which major nucleation flux bypasses the thermodynamic saddle point were clarified, and both the discrepancy in the attachment rates of two species and the nonuniformity of the direction of nucleation flux were found to be the major causes of the ridge crossing.

(3) Binary nucleation reduces kinetically to a single component nucleation when the attachment rate for one of two species tends to vanish.

(4) The ridge crossing reported by Wyslouzil and Wilemski [13] was well explained on the basis of the present theory.

ACKNOWLEDGMENTS

J.-S.L. expresses his sincere gratitude to his doctoral supervisor, the late Professor K. Nishioka of the University of Tokushima, for guiding him to the theory of kinetic nucle-

ation. J.-S.L. wishes to thank Professor G. Wilemski for fully reading the manuscript and giving very essential comments. J.-S.L. also wishes to thank Dr. I. Kusaka, Dr. K. Ohno, and Dr. T. Takeuchi for helpful discussions, and the Japanese Ministry of Education for granting him the Monbusho scholarship. I.L.M. appreciates the JSPS support in accordance with the JSPS visiting researcher program. This work was supported by JSPS Research for the Future Program in the Area of Atomic Scale Surface and Interface Dynamics under the Project ''Dynamic behavior of grown surface and interface, and atomic scale simulation,'' and partially by the Satellite Venture Business Laboratory of Tokushima University.

[1] J. S. Langer, Phys. Rev. Lett. **21**, 973 (1968).
[2] K. Binder and D. Stauffer, Adv. Phys. **25**, 343 (1976).
[3] A. Laaksonen, V. Talanquer, and D. W. Oxtoby, Annu. Rev. Phys. Chem. **46**, 489 (1995).
[4] S. Qi and Z.-G. Wang, Phys. Rev. Lett. **76**, 1679 (1996).
[5] R. Reigada, F. Sagues, I. M. Sokolov, J. M. Sancho, and A. Blumen, Phys. Rev. Lett. **78**, 741 (1997).
[6] M. Rao and S. Sengupta, Phys. Rev. Lett. **78**, 741 (1997).
[7] H. Reiss, J. Chem. Phys. **18**, 840 (1950).
[8] J. O. Herschfelder, J. Chem. Phys. **35**, 2690 (1974).
[9] G. Wilemski, J. Chem. Phys. **62**, 3763 (1975).
[10] D. Stauffer, J. Aerosol Sci. **7**, 319 (1976).
[11] A. L. Greer, P. V. Evans, R. G. Hamerton, D. K. Shangguan, and K. F. Kelton, J. Cryst. Growth **99**, 38 (1990).
[12] R. McGraw, J. Chem. Phys. **102**, 2098 (1995).
[13] B. E. Wyslouzil and G. Wilemski, J. Chem. Phys. **103**, 1137 (1995).
[14] H. Trinkaus, Phys. Rev. B **27**, 7372 (1983).
[15] G. Shi and J. H. Seinfeld, J. Chem. Phys. **93**, 9033 (1990).
[16] D. T. Wu, J. Chem. Phys. **99**, 1990 (1993).
[17] L. M. Berezhkovskii and V. Yu. Zitserman, J. Chem. Phys. **102**, 3331 (1995).
[18] S. M. Kreidenweis, R. C. Flagan, J. H. Seinfeld, and K. Okuyama, J. Aerosol Sci. **20**, 585 (1989).
[19] J.-S. Li, K. Nishioka, and I. L. Maksimov, J. Chem. Phys. **107**, 460 (1997).
[20] J. Lothe and G. M. Pound, J. Chem. Phys. **36**, 2080 (1962).
[21] P. M. Morse and H. Feshbach, *Methods of Theoretical Physics* (McGraw-Hill, New York, 1953), Part I, pp. 8–31.
[22] K. Nishioka, Phys. Rev. E **52**, 3263 (1995).
[23] K. Nishioka and I. L. Maksimov, J. Cryst. Growth **163**, 1 (1996).
[24] B. E. Wyslouzil and G. Wilemski, J. Chem. Phys. **105**, 1090 (1996).